REPORT DOCUMENTATION PAGE

Form Approved
OMB NO. 0704-0188

1. AGENCY USE ONLY (Leave Blank)	2. REPORT DATE	3. REPORT TYPE AND DATES COVERED
	Sept. 20, 2006	Final technical, 6/16/2003-6/15/2006

4. TITLE AND SUBTITLE
Electromagnetically induced transparency in semiconductors

5. FUNDING NUMBERS
DAAD19-03-1-0137

6. AUTHOR(S)
Hailin Wang

7. PERFORMING ORGANIZATION NAME(S) AND ADDRESS(ES)
University of Oregon, Research Service and Administration, Eugene, OR97403

8. PERFORMING ORGANIZATION REPORT NUMBER

9. SPONSORING / MONITORING AGENCY NAME(S) AND ADDRESS(ES)
U. S. Army Research Office
P.O. Box 12211
Research Triangle Park, NC 27709-2211

10. SPONSORING / MONITORING AGENCY REPORT NUMBER
44930.1-PH

11. SUPPLEMENTARY NOTES
The views, opinions and/or findings contained in this report are those of the author(s) and should not be construed as an official Department of the Army position, policy or decision, unless so designated by other documentation.

12 a. DISTRIBUTION / AVAILABILITY STATEMENT
Approved for public release; distribution unlimited.

12 b. DISTRIBUTION CODE

13. ABSTRACT (Maximum 200 words)

This final technical report summarizes research supported by ARO in two areas: electromagnetically induced transparency (EIT) from electron spin coherence and cavity QED with nitrogen vacancy (NV) centers in diamond nanocrystals. We have developed three different schemes to realize EIT using electron spin coherence in semiconductor quantum wells. The three schemes include the use of V-type three-level systems via heavy hole excitonic transitions in an external magnetic field in the Voigt geometry, the use of V-type three-level systems via light hole excitonic transitions in a waveguide geometry and in the absence of an external magnetic field, and the use of a lamda-type three-level system in a mixed-type quantum well structure. We have achieved the breakthrough of realizing the strong coupling regime in cavity QED by coupling NV centers in diamond nanocrystals to whispering gallery modes in a deformed fused silica microsphere. In addition, our improved understanding on how electron spin coherence contributes to nonlinear optical processes in semiconductors has also led to the demonstration of a spin manipulation scheme that controls both the amplitude and phase of electron spin precessions.

14. SUBJECT TERMS
Electromagnetically induced transparency (EIT), spin coherence, cavity QED, nitrogen vacancy (NV) centers, whispering gallery mode (WGM), quantum well

15. NUMBER OF PAGES

16. PRICE CODE

17. SECURITY CLASSIFICATION OR REPORT	18. SECURITY CLASSIFICATION ON THIS PAGE	19. SECURITY CLASSIFICATION OF ABSTRACT	20. LIMITATION OF ABSTRACT
UNCLASSIFIED	**UNCLASSIFIED**	**UNCLASSIFIED**	**UL**

NSN 7540-01-280-5500

Standard Form 298 (Rev.2-89)
Prescribed by ANSI Std. 239-18
298-102

Enclosure 1

Final Progress Report

Electromagnetically induced transparency in semiconductors

June 16, 2003 to June 15, 2006

Principal Investigator:	Hailin Wang Professor Department of Physics University of Oregon Eugene, OR 97403 Voice 541-346-4758 Fax 541-346-4315 hailin@uoregon.edu
Institution:	University of Oregon Research Service and Administration Eugene, OR 97403-5215

Grant Number:	DAAD19-03-1-0137
ARO Proposal Number:	44930-PH
ARO Tech. representative:	Dr. T.R. Govindan

TABLE OF CONTENTS

1. Statement of problems studied

a) Electromagnetically induced transparency in semiconductors

We have pursued an experimental program to realize electromagnetically induced transparency (EIT) in semiconductors. EIT is a phenomenon that exploits destructive interference induced by a nonradiative quantum coherence to render an opaque medium transparent. EIT can enable important applications in both classical (e.g., optical buffers) and quantum information processing (e.g., quantum memory and quantum repeaters).

A main challenge for realizing EIT-based applications is to identify and develop suitable material systems with appropriate energy-level structures and robust quantum coherences. Most forms of quantum coherences in semiconductors are fragile, with decoherence time shorter than 100 ps even at low temperature. Recent experimental studies, however, have demonstrated that electron spin coherence in semiconductors can remain robust at room temperature and that spin coherence can be transported across semiconductor interfaces. Our research efforts have focused on the use of robust electron spin coherence for EIT in semiconductor nanostructures.

b) Cavity QED with NV centers and silica microspheres

Cavity QED in the strong-coupling regime, characterized by a reversible exchange of energy between a 2-level system and a cavity mode, has played a key role in many quantum information processes. The coherent energy exchange occurs at the level of single quanta and can induce controlled spin-photon, spin-spin, and photon-photon entanglement. In order to use the strong-coupling process for quantum control of entanglement in a solid-state environment, the cavity QED system needs to feature a robust spin coherence, since coupling to the surrounding environment leads to rapid decay of most other forms of quantum coherences. Among various solid-state spin systems, nitrogen vacancy (NV) centers in diamond have emerged as one of the most promising candidates. A NV center consists of a substitutional nitrogen atom and an adjacent vacancy in diamond. These defect centers can feature near unity quantum efficiency, a homogenous linewidth as small as 50 MHz, and an electron spin decoherence time exceeding 50 μs at room temperature.

We have developed a composite nanocrystal-microsphere system, in which NV centers in diamond nanocrystals are coupled to a whispering gallery mode (WGM) in a silica microsphere. The composite nanocrystal-microsphere system combines and takes advantage of both the exceptional spin properties of NV centers and the ultra high quality factor of silica microspheres. The normal mode splitting observed in the composite nanocrystal-microsphere system demonstrates the strong-coupling between a WGM and single NV centers in diamond nanocrystals.

2. Summary of the most important results

1) Electromagnetically induced transparency in semiconductors

We have developed three different schemes to realize EIT using electron spin coherence in semiconductor quantum wells (QWs). The three schemes include the use of V-type three-level systems via heavy (HH) excitonic transitions in an external magnetic field in the Voigt geometry, the use of V-type three-level systems via light hole (LH) excitonic transitions in a waveguide geometry and in the absence of an external magnetic field, and the use of a Λ-type three-level system in a mixed-type QW structures.

Interband dipole optical transitions near the band edge of semiconductors such as a GaAs QW are characterized by transitions between the doubly degenerate conduction bands with s_z=1/2 and –1/2 and the doubly degenerate HH and LH valence bands with j_z=±3/2 and ±1/2, respectively (see Fig. 1a). The two HH transitions share no common states. Electron spin coherence can be induced via HH transitions in the presence of an external magnetic field in the Voigt geometry. Alternatively, we can take advantage of the unique polarization selection rule for the LH transitions in a QW waveguide to induce electron spin coherence in the absence of an external magnetic field. As shown in Fig. 1a, the two electron spin states in the s-like conduction band can couple to a common LH valence band via two dipole optical transitions. One of the transitions is driven by an optical field polarized along the z-axis (the growth direction). The other can be driven by either σ+ or σ– polarized optical fields. The field polarized along the z-axis has to propagate in the plane of the QW (the x-y plane), i.e., in the waveguide. EIT via LH transitions can be realized by using a signal beam polarized along the z-axis and a control beam polarized along the x-axis. Both the signal and the control can propagate along the y-axis in the waveguide (co-propagating configuration). Alternatively, the control beam can propagate along the z-axis and perpendicular to the waveguide (orthogonal configuration, see Fig. 1b).

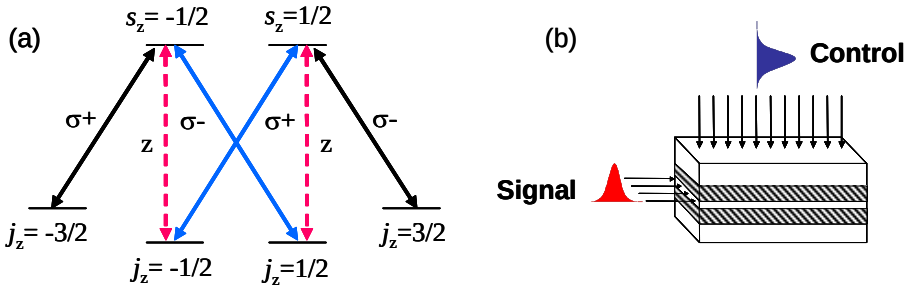

Fig. 1 (a) Schematic of energy level structures and optical selection rules for HH and LH transitions in a GaAs QW. (b) Schematic of EIT in a waveguide geometry, in which a control pulse controls the propagation of a signal pulse in the waveguide.

(a) EIT from electron spin coherence via HH transitions

Figures 2a and 2b show the energy level structure for the HH transition in a GaAs QW subject to a DC magnetic field along the x-axis. For the conduction band, s_x is a good quantum number. For the valence band, j_z remain approximately a good quantum number, leading to the selection rule for circularly polarized and linearly polarized fields shown in Figs. 2a and 2b. Electron spin coherence, i.e. coherent superposition of s_x=1/2 and -1/2 states, can be excited with two laser beams with the same circular or orthogonal linear polarization. For EIT, the control and signal need to couple to different transitions, which can be accomplished by using two laser beams with orthogonal linear polarizations (see Fig. 2b).

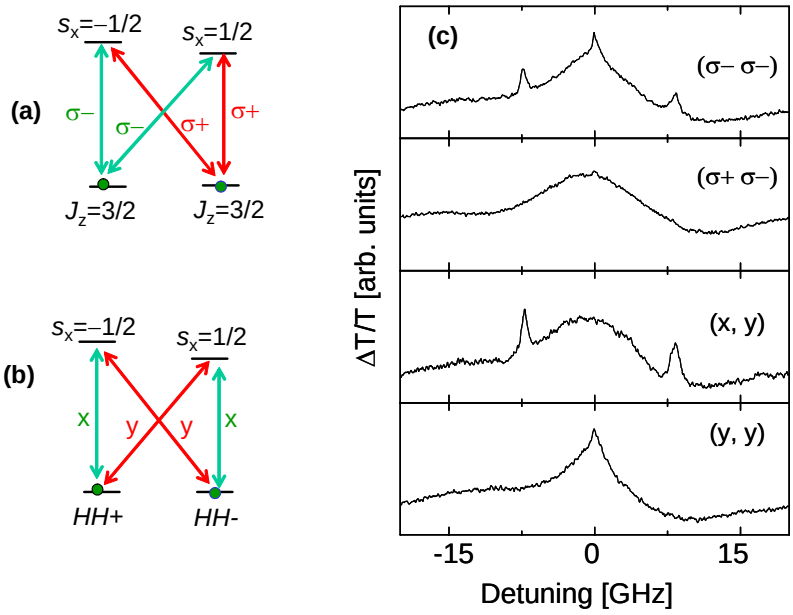

Fig. 2 (a) and (b) Polarization selection rule of HH transitions subject to a DC magnetic field along the x-axis. (c) Differential transmission spectra show the polarization selection rule for the coherent Zeeman resonance. The data were obtained at T = 10K and B= 2T in a 13 nm GaAs QW.

We have demonstrated the basic destructive interference process underlying the HH EIT scheme using differential transmission (DT) with CW control and signal beams [1]. In these studies, the control and signal excite an electron spin coherence. Destructive interference induced by the spin coherence then leads to a sharp resonance in the DT spectrum measured by the signal beam. Figures 2c show DT spectra obtained at B= 2T with various polarization configurations. The DT response was measured as a function of the detuning between the control and signal, with the control frequency fixed. Sharp induced resonances occur in the DT spectra away from the zero detuning when the control and signal have the same circular or the orthogonal linear

polarization, as expected from the polarization selection rule shown in Figs. 2a and 2b. The spectral position and linewidth of these resonances are determined by the electron spin splitting and the lifetime of the electron spin coherence, respectively. These coherent Zeeman resonances arise from destructive interference induced by the electron spin coherence. The same, but complete destructive interference, leads to EIT.

(b) EIT from electron spin coherence via LH transitions

For the LH transition, it is possible to couple the $s_z = \pm 1/2$ conduction bands to a common LH valence band via two dipole transitions, as shown in Fig. 1a. To demonstrate the basic destructive interference process underlying the LH EIT scheme, we shown in Fig. 3a the DT spectrum obtained at T=50 K in a 17.5 nm GaAs waveguide [2]. A sharp resonance occurs at the zero control-signal detuning. To confirm that this resonance arises from destructive interference induced by the electron spin coherence, we applied to the QW waveguide an external magnetic field along the z-axis. The external magnetic field induces energy splitting in both the conduction and valence bands, but does not affect the dipole selection rule (this would not be the case if the external magnetic field were applied along the x- or y-axis). Figure 3b shows the DT response obtained at B=0.25 T and with otherwise identical conditions. Induced resonances now occur symmetrically away from the zero detuning. The spectral position of the two induced resonances corresponds to the electron spin splitting, demonstrating that these resonances arise from destructive interference induced by the electron spin coherence.

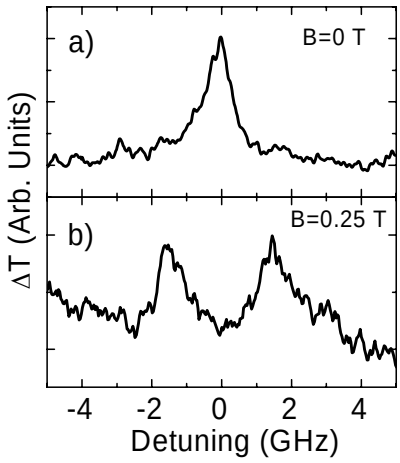

Fig. 3 Differential transmission spectra demonstrate destructive interference underlying the LH EIT scheme. The data were obtained at T=50 K in a 17.5 nm GaAs QW waveguide. Both TE-polarized control and TM-polarized signal propagate along the waveguide. (a) B=0 and (b) B=0.25 T. The external magnetic field is applied along the z-axis.

(c) EIT from electron spin coherence in a mixed-type quantum well

There are two limitations for the EIT scheme discussed above. First of all, absorption of the control beam is unavoidable in such a scheme. Secondly, the lifetime of the electron spin coherence is limited by the radiative lifetime. A more ideal system, which overcomes these limitations, is a Λ-type 3-level system, in which the two lower states are the electron spin states.

To realize a Λ-type 3-level system, we have used a GaAs/AlAs mixed-type QW (MTQW) system. As shown in Fig. 4a, the MTQW structure consists of narrow and wide GaAs wells separated by an AlAs barrier. Electrons photoexcited above the band gap in the narrow well (NW) can thermalize and transfer via the X-valley in the AlAs barrier to the conduction band of the wide well (WW). The holes, however, remain confined in the NW, preventing recombination with the electrons. Optical excitation of electron-hole pairs in the NW controls the electron density that collects in the WW. For electrons in the WW, a Λ-type 3-level system can be realized by coupling the spin-up and spin-down electron states to a trion state X^-, defined as an exciton bound to an electron (see Fig. 4b). Using a MTQW sample grown by J. Prineas's group at the University of Iowa according to our design, we have demonstrated the coherent Zeeman resonance from electron spin coherence in the Λ-type 3-level system [3], which can be viewed as a precursor to EIT.

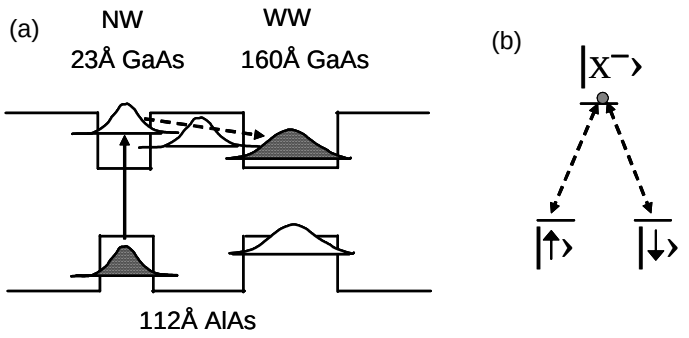

Fig. 4 (a) Schematic of a mixed-type GaAs/AlAs quantum well structure. (b) A Λ-type three-level system formed by spin-up and spin-down electron states coupling to a trion state, X^-, via two dipole optical transitions.

2) Cavity QED with NV centers and silica microspheres

We have achieved the breakthrough of realizing the strong coupling regime in cavity QED by coupling NV centers in diamond nanocrystals to WGMs in a deformed fused silica microsphere [4]. The demonstration of a strong-coupling cavity QED system with NV centers opens the door to employing robust electron spin coherence in the strong-coupling cavity QED regime. Specifically, strong-coupling cavity QED systems with NV centers featuring μs spin decoherence time at room temperature provide us a highly promising system to explore important quantum information processes such as distributed quantum networks and spin entanglement.

For our studies, type 1b diamond nanocrystals synthesized under high pressure and high temperature and with an average size of 75 nm were obtained from de Beers. The nanocrystals were irradiated with electron beams and annealed in vacuum at 900 K to create NV centers. Diamond nanocrystals were then deposited onto the surface of a silica microsphere using solution deposition. Figure 5a shows the image of a sphere used in our study. Figure 5b shows a

confocal microscopic image of nanocrystals dispersed on the surface of a silica sphere, for which only a ring-shaped section of the sphere surface is in focus (a portion of the ring is displayed in Fig. 5b). Figure 5c shows the PL spectra from individual NV centers.

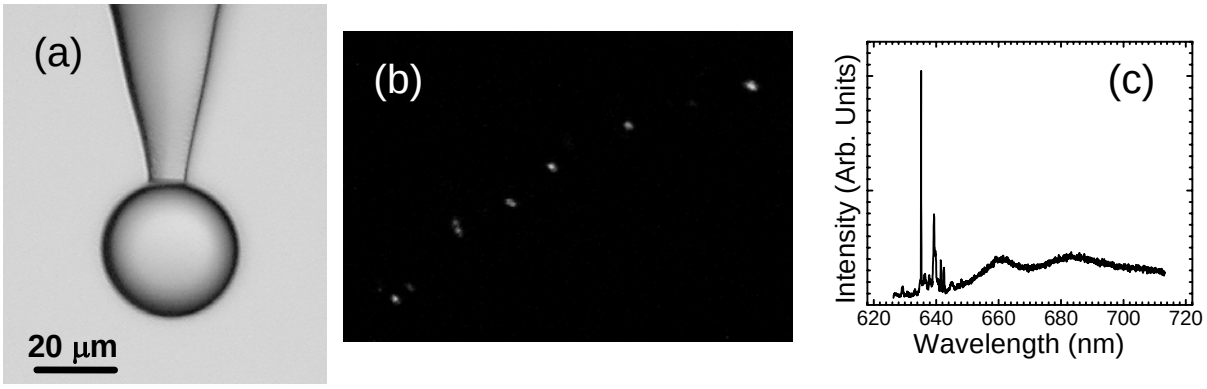

Fig. 5 (a) Image of a silica microsphere. (b) Image of NV centers on the surface of a silica microsphere. (c) PL spectra from single NV centers (T=5 K).

A technical difficulty for cavity QED with WGM resonators is the excitation of high-Q WGMs at low temperature. For ease of operation, we have developed a technique of free-space evanescent coupling using nearly spherical but non-axisymmetric microspheres. Critical to our experimental success is that this technique allowed us to explore a large number of microspheres to determine the suitable parameters and conditions necessary for achieving strong coupling.

We match a WGM resonance with the optical transition frequency in a NV center by varying the detuning between the WGM and the NV center via temperature tuning. Figure 6a shows the resonant scattering spectra of a nanocrystal-microsphere system obtained near λ=634.2 nm (sphere diameter ~ 35 μm) and at temperatures ranging from 6 K to 12.4 K. Two normal mode branches corresponding to atom-like and cavity-like modes are indicated in Fig. 3a by blue and red arrows, respectively. Unlike cavity QED systems based on the use of semiconductor nanocrystals, the normal mode resonances in Fig. 6a show no noticeable spectral fluctuations under repeated measurements.

For a more detailed analysis of the normal mode coupling in Fig. 6a, we plot in Figs. 6b and 6c the expanded scan obtained at T=6 K and T=9 K, for which the WGM and the NV center are detuned and nearly resonant, respectively. Figures 6d and 6e plot the spectral position and linewidth of the two normal modes obtained in Fig. 6a as a function of the temperature. Figure 6d shows the avoided crossing of the spectral positions of the two normal modes. Figure 6e shows that the linewidth of the normal modes approaches the average of the individual linewidth for the NV center ($\gamma/2\pi$ = 25 MHz) and the WGM ($\kappa/2\pi$ = 50 MHz), when the NV center is

nearly resonant with the WGM. These behaviors demonstrate conclusively that the cavity QED system has reached the strong coupling regime.

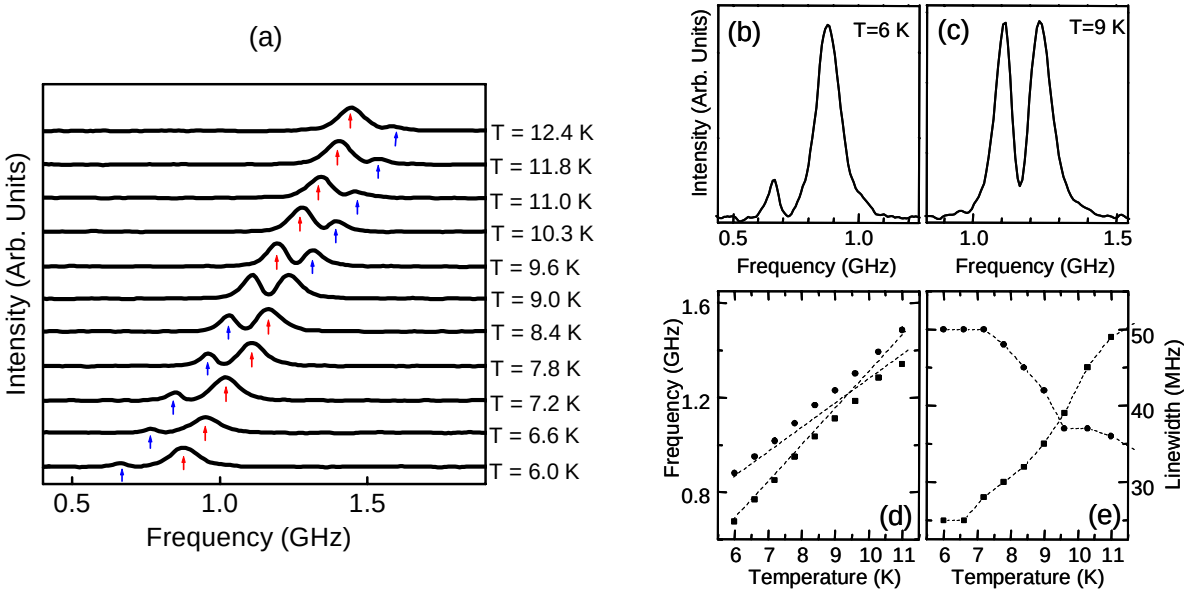

Fig. 6 (a) Resonant scattering spectra of a cavity QED system, where the cavity-like and atom-like modes are indicated by red and blue arrows, respectively. (b, c) The expanded scan of normal resonances obtained at T=6 K and T=9 K. (d, e) The spectral position and linewidth of the two normal modes as a function of the temperature. The circles and squares are for the upper and lower frequency normal modes, respectively. The dashed lines are a guide to the eye.

For a more detailed analysis of the normal mode coupling in Fig. 6a, we plot in Figs. 6b and 6c the expanded scan obtained at T=6 K and T=9 K, for which the WGM and the NV center are detuned and nearly resonant, respectively. Figures 6d and 6e plot the spectral position and linewidth of the two normal modes obtained in Fig. 6a as a function of the temperature. Figure 6d shows the avoided crossing of the spectral positions of the two normal modes. Figure 6e shows that the linewidth of the normal modes approaches the average of the individual linewidth for the NV center ($\gamma/2\pi$ = 25 MHz) and the WGM ($\kappa/2\pi$ = 50 MHz), when the NV center is nearly resonant with the WGM. These behaviors demonstrate conclusively that the cavity QED system has reached the strong coupling regime.

3) Nonlinear optical processes of electron spin coherences

To further optimize the EIT process, we have carried out extensive experimental studies to investigate how electron spin coherence contributes to nonlinear optical processes in semiconductors and especially what are the roles of manybody interactions. Experimental

studies of quantum beats in optical absorption induced by electron spin coherence have shown that simple atomic-like descriptions of electron spin coherence fail completely in semiconductors [5]. In these studies, we spectrally separated contributions from localized and mobile excitons in GaAs QWs. Absorption quantum beats occur for strongly localized excitons, but nearly vanish for mobile excitons in the third order nonlinear optical response. Pronounced quantum beats for mobile excitons emerge in an unusual fifth order process. A qualitative analysis of the experimental results based on the use of a *N*-exciton eigenstate model further elucidates how the manifestation of electron spin coherence in the excitonic nonlinear optical response depends crucially on the underlying exciton-exciton interactions, leading to a fundamental understanding of nonlinear optics of electron spin coherence in semiconductors.

We have also developed and used a technique of nearly degenerate time-resolved Faraday rotation (TRFR) to probe coherent nonlinear optical processes associated with the electron spin coherence in semiconductors [6]. In the nearly degenerate TRFR, we measure the TRFR response as a function of the detuning between a pump and a probe near an exciton resonance. We show that manybody exciton-exciton interactions strongly modify the coherent nonlinear optical response through the coupling of the spin coherence to bound as well as unbound two-exciton states. These couplings are revealed by distinct lineshapes in spectral TRFR responses, even though the corresponding temporal TRFR response shows no apparent effects of manybody interactions.

The improved understanding on how electron spin coherence contributes to nonlinear optical processes has led to the development and demonstration of a spin manipulation scheme that controls the amplitude as well as the phase of the quantum beats from electron spin coherence [7]. The spin manipulation scheme exploits the relative phase between relevant Larmor precessions by tipping the precessing spin at a specified time. This scheme also takes advantage of the underlying exciton-exciton interactions inherent in a semiconductor and can be more effective in an excitonic system than in a corresponding atomic-like system.

4) Decoherence in self-assembled quantum dots

We have carried out detailed experimental studies on fundamental decoherence processes in self-assembled CdSe quantum dots. The primary purpose of these studies is to compare intrinsic decoherence processes between self-assembled quantum dots and chemically synthesized quantum dots and also to lay the ground work for the use of these quantum dots in later EIT studies.

The experimental studies, which are based on the use of high-resolution spectral hole burning, have shown that the self-assembled CdSe quantum dots feature intrinsic homogeneous linewidth that is comparable to the chemically synthesized CdSe quantum dots [8]. In addition,

the homogeneous linewidth in these CdSe quantum dots is nearly the same as that in self-assembled InAs quantum dots. This is somewhat surprising since electron-phonon interactions in II-VI semiconductors such as CdSe are much stronger than those in III-V semiconductors such as GaAs or InAs. Our experimental results have provided valuable information for formulating a theoretical description of intrinsic decoherence processes in semiconductors.

3. Publication

JOURNAL ARTICLES:

Phedon Palinginis and Hailin Wang, "Vanishing and emerging of absorption quantum beats from electron spin coherence in GaAs quantum wells," Phys. Rev. Lett. 92, 037402 (2004).

Mark Phillips and Hailin Wang, "Exciton spin coherence and electromagnetically induced transparency in the transient optical response of GaAs quantum wells," Phys. Rev. B69, 115337 (2004).

Phedon Palinginis, Hailin Wang, Serguei Gupalov, D.S. Citrin, M. Dobrowolska, and J. Furdyna, "Exciton dephasing in self-assembled CdSe quantum dots," Phys. Rev. B. 70, 073302 (2004).

Phedon Palinginis and Hailin Wang, "Coherent Raman resonance from electron spin coherence in GaAs quantum wells," Phys. Rev. B70, 153307 (2004).

Susanta Sarkar, P.C. Ku, C. J. Chang-Hasnain, N.H. Kwong, R. Binder, and Hailin Wang, "Inducing electron spin coherence in a quantum well waveguide: Spin coherence without spin precession," Phys. Rev. B72, 035343 (2005).

Yumin Shen, A. Goebel, G. Khitrova, H. Gibbs, and Hailin Wang, "Nearly degenerate time-resolved Faraday rotation in semiconductors," Phys. Rev. B72, 233307 (2005).

Young-Shin Park, Andrew Cook, and Hailin Wang, "Cavity QED with diamond nanocrystals and silica microspheres," Nano Lett. 6, 2075 (2006).

Shannon O'Leary, Hailin Wang, and John Prineas, "Coherent Zeeman Resonance from Electron Spin Coherence in a Mixed-Type GaAs/AlAs Quantum Well," Submitted to Opt. Lett. (2006).

Yumin Shen, A. Goebel, and Hailin Wang, "Control of quantum beats from electron spin coherence in quantum wells," submitted to Phys. Rev. Lett. (2006).

BOOK CHAPTER:

Mark Phillips and Hailin Wang, "*Electromagnetically induced transparency in semiconductors,*" in Nonequilibrium Dynamics of Semiconductor and Nanostructures, Edited by K.T. Tzen, (Marcel Dekker, New York 2005).

4. Scientific Personnel

Phedon Palinginis (graduate student)
Susanta Sarkar (graduate student)
Yumin Shen (graduate student)
Yao Li (graduate student)
Hailin Wang (PI)

Phedon Palinginis graduated with PhD in physics in April 2004.
Susanta Sarkar graduated with PhD in physics in June 2006.

5. Report of inventions

No patents were filed.

6. Bibliography

1) T Phedon Palinginis and Hailin Wang, "Coherent Raman resonance from electron spin coherence in GaAs quantum wells," Phys. Rev. B70, 153307 (2004).

2) Susanta Sarkar, P.C. Ku, C. J. Chang-Hasnain, N.H. Kwong, R. Binder, and Hailin Wang, "Inducing electron spin coherence in a quantum well waveguide: Spin coherence without spin precession," Phys. Rev. B72, 035343 (2005).

3) Shannon O'Leary, Hailin Wang, and John Prineas, "Coherent Zeeman Resonance from Electron Spin Coherence in a Mixed-Type GaAs/AlAs Quantum Well," Submitted to Opt. Lett. (2006).

4) Young-Shin Park, Andrew Cook, and Hailin Wang, "Cavity QED with diamond nanocrystals and silica microspheres," Nano Lett. 6, 2075 (2006).

5) Phedon Palinginis and Hailin Wang, "Vanishing and emerging of absorption quantum beats from electron spin coherence in GaAs quantum wells," Phys. Rev. Lett. 92, 037402 (2004).

6) Yumin Shen, A. Goebel, G. Khitrova, H. Gibbs, and Hailin Wang, "Nearly degenerate time-resolved Faraday rotation in semiconductors," Phys. Rev. B72, 233307 (2005).

7) Yumin Shen, A. Goebel, and Hailin Wang, "Control of quantum beats from electron spin coherence in quantum wells," submitted to Phys. Rev. Lett. (2006).

8) Phedon Palinginis, Hailin Wang, Serguei Gupalov, D.S. Citrin, M. Dobrowolska, and J. Furdyna, "Exciton dephasing in self-assembled CdSe quantum dots," Phys. Rev. B. 70, 073302 (2004